HNF4g invalidation prevents diet-induced obesity via intestinal lipid malabsorption

Marine Halbron, Olivier Bourron, Fabrizio Andreelli, Cecile Ciangura, Sophie Jacqueminet, Marc Popelier, Frederic Bosquet, Stephanie Rouanet, Chloe Amouyal, Agnes Hartemann

Accepted Manuscript published as JOE-21-0092.R1. Accepted for publication: 12-Oct-2021

HNF4g invalidation prevents diet-induced obesity via intestinal lipid malabsorption

Sami Ayari[1], Eva Gil-Iturbe[1], Léa le Gléau[1], Céline Osinski[1], Nathalie Kapel[2], Hedi Antoine Soula[1], Armelle Leturque[1], Fabrizio Andreelli[1, 3,4], Karine Clément[1,3], Patricia Serradas[1], Agnès Ribeiro[1*]

1- Sorbonne Université, INSERM, Nutrition and obesities: systemic approaches, F-75013 Paris, France
2- AP-HP Hôpital Pitié-Salpêtrière-Charles Foix, Functional Coprology Department, F-75013 Paris, France
3- AP-HP Hôpital Pitié-Salpêtrière-Charles Foix, Nutrition Department, F-75013 Paris, France
4- AP-HP Hôpital Pitié-Salpêtrière-Charles Foix, Diabetology-Metabolism Department, F-75013 Paris, France

Present address:

E G-I: Department of Psychiatry – Division of Molecular Therapeutics, Columbia University Irving Medical Center, New York, NY, USA

***Corresponding author:** Agnès Ribeiro, Sorbonne Université, INSERM, Nutrition and obesities: systemic approaches, F-75013 Paris, France – e-mail: agnes.ribeiro@sorbonne-universite.fr

Short title: HNF4G and lipid malabsorption in intestine

Word count: ~~4409~~ 4895 words

Keywords: HNF-4gamma, intestine, obesity, lipid malabsorption, GLP-1, high-fat/high fructose diet.

Abstract

Changes in dietary habits have occurred concomitantly with a rise of type 2 diabetes (T2D) and obesity. Intestine is the first organ facing nutrient ingestion and has to adapt its metabolism with these dietary changes. HNF-4γ, a transcription factor member of the nuclear receptor superfamily and mainly expressed in intestine has been suggested involved in susceptibility to T2D. Our aim was to investigate the role of HNF-4γ in metabolic disorders and related mechanisms. *Hnf4g*$^{-/-}$ mice were fed high-fat/high-fructose (HF-HF) diet for 6 weeks to induce obesity and T2D. Glucose homeostasis, energy homeostasis in metabolic cages, body composition and stool energy composition, as well as gene expression analysis in jejunum were analyzed. Despite an absence of decrease in calorie intake, of increase in locomotor activity or energy expenditure, *Hnf4g*$^{-/-}$ mice fed HF-HF are protected against weight gain after 6 weeks of HF-HF diet. We showed that *Hnf4g*$^{-/-}$ mice fed HF-HF display an increase in fecal calorie loss, mainly due to intestinal lipid malabsorption. Gene expression of lipid transporters, *Fatp4* and *Scarb1* and of triglyceride-rich lipoprotein secretion proteins, *Mttp* and *ApoB* are decreased in gut epithelium of *Hnf4g*$^{-/-}$ mice fed HF-HF, showing the HNF-4γ role in intestine lipid absorption. Furthermore, plasma GLP-1 and jejunal GLP-1 content are increased in *Hnf4g*$^{-/-}$ mice fed HF-HF, which could contribute to the glucose intolerance protection. The loss of HNF-4γ leads to a protection against a diet-induced weight gain and to a deregulated glucose homeostasis, associated with lipid malabsorption.

 Accepted Manuscript published as JOE-21-0092.R1. Accepted for publication: 12-Oct-2021

Introduction

HNF-4 belongs to the nuclear receptor superfamily and in mammals, two paralog genes encode the HNF-4α and HNF-4γ forms. HNF-4α is expressed in liver, kidney, pancreas and intestine (Benoit et al., 2006). Numerous studies *in vivo* and *in vitro* have shown that HNF-4α plays pleiotropic roles in liver functions and is a central transcription factor at the crossroads between epithelial morphogenesis and functions (Battle et al., 2006; Hwang-Verslues and Sladek, 2010; Ribeiro et al., 2007). Intestinal mice *Hnf4a* gene invalidation induces impairment of intestinal epithelium homeostasis, regeneration, cell architecture and fatty acid uptake (Cattin et al., 2009; Frochot et al., 2012; Montenegro-Miranda et al., 2020; Saandi et al., 2013).

HNF-4γ is expressed mainly in intestine and colon, in kidney and to a lesser extent in pancreas (Bookout et al., 2006), being almost absent from liver (Plengvidhya et al., 1999; Taraviras et al., 2000). HNF-4γ is highly expressed during intestine specification (Li et al., 2009). Recently, a novel variant of HNF-4γ, designated HNF-4γ2 was found to promote transactivation capacity and hepatic function of dedifferentiated hepatoma cells better than HNF-4α (Sasaki et al., 2018). Furthermore, an integrative multi-omics analysis in intestinal organoids highlighted HNF-4γ as a major driver of enterocyte differentiation (Lindeboom et al., 2018). It is noteworthy that the physiological role of HNF-4γ was much less studied than that of HNF-4α and there is a lack of information on HNF-4γ. Using constitutive *Hnf4g* gene invalidation model fed control diet, we demonstrated that loss of HNF-4γ leads to an overproduction of GLP-1, leading to an exaggerated glucose-induced insulin secretion that improves glucose tolerance of *Hnf4g*$^{-/-}$ mice through an increase in GLP-1 incretin effect and a trophic impact on pancreatic β-cell mass (Baraille et al., 2015). HNF-4γ loss impacts the abundance of β-cells but not on their insulin secretory capacity and led to a resistance to streptozotocin, a β-cell cytotoxic drug (Baraille et al., 2015). The role of HNF-4γ deserves thus further attention in the susceptibility to type 2 diabetes (T2D) using appropriate mouse model.

T2D is one of numerous co-morbidities associated with obesity as well as cardiovascular diseases (Stahel et al., 2020). The duration and the amplitude of the post-prandial peak of circulating triglyceride rich lipoproteins (TRL) from intestinal origin are risk of cardiovascular diseases (Bansal et al., 2007; Duez et al., 2008; Hsieh et al., 2008; Nordestgaard et al., 2007). Furthermore, changes of intestinal TRL secretion have been reported in the context of insulin resistance or diabetes, in animal models (Haidari et al., 2002; Vine et al., 2007) and in humans (Duez et al., 2006). There is evidence for an increased basal rate of intestine-specific apolipoprotein (apo)B-48-containing lipoprotein secretion in insulin resistance and T2D (Adeli and Lewis, 2008). Inversely, insulin reduces TRL and apoB-48 secretion (Levy et al., 1996). In insulin resistant fructose-fed hamsters, *de novo* lipogenesis is enhanced (Haidari et al., 2002; Lewis et al., 2005). Hyperinsulinemic insulin-resistant human subjects display increased production rates of intestinal apoB48-containing lipoproteins (Duez et al., 2006), and in individuals with type 2 diabetes, intestinal chylomicron production is resistant to insulin's acute suppressive effects (Nogueira et al., 2012). The relationships between T2D and lipid metabolism in the context of *hnf4g* invalidation deserve further investigation.

Changes in dietary habits, including increments in calorie and saturated fatty acid intakes, have occurred concomitantly with a rise of T2D and obesity (Shikany and White, 2000). Intestine has to adapt its metabolism to accommodate the increased lipid intake.

The intestine ensures the transport of alimentary fat, which is the most calorie-dense nutrient. Enterocytes ensure the transfer of dietary lipids to the organism through complex processes (Williams, 2008). Triglycerides (TG) are hydrolyzed mainly by pancreatic enzymes into fatty acids and monoglycerides. The uptake of fatty acids occurs by passive diffusion and by a saturable/ protein-mediated mechanism comprising the fatty acid translocase (CD36), the fatty acid-binding protein from the plasma membrane (FABPpm), as well as the fatty acid transport protein (FATP) family (Gimeno et al., 2003; Nordestgaard et al., 2007; Stahl et al., 1999). After

 Accepted Manuscript published as JOE-21-0092.R1. Accepted for publication: 12-Oct-2021

resynthesis within the endoplasmic reticulum membrane, TG are used to form chylomicrons, the intestine-specific postprandial form of TRL, which will be secreted into the lymph and then directed toward circulation. The assembly of one TRL results from the fusion between one apoB molecule, which is necessary for their formation, and one independently formed TG droplet (Davidson and Shelness, 2000). The microsomal TG transfer protein (MTP) has a prominent role in chylomicron assembly, ensuring the lipidation-dependent stabilization of apoB and the transfer of lipids to the TG droplet in the endoplasmic reticulum lumen (Iqbal and Hussain, 2009). During the postprandial period, TG are also transiently stored in enterocytes, as cytosolic lipid droplets surrounded by proteins such as ADRP, which can be subsequently hydrolyzed to reenter the secretory pathway (Robertson et al., 2003). Thus perturbations of their basal level of expression and/or their nutrient-dependent modulation should interfere with the enterocyte function of dietary lipid absorption and would reveal functional role of HNF-4γ in intestinal absorption of lipids.

To test the hypothesis of a role of HNF-4γ in metabolic disorders related to intestine, we submitted the constitutive *Hnf4g* gene invalidation model to a high-fat/high-fructose (HF-HF) diet for 6 weeks, in order to induce obesity and T2D.

Materials and methods

Animals and treatments

Total and constitutive *Hnf4g* gene invalidation was as previously described (Baraille et al., 2015; Gerdin et al., 2006). Heterozygote *Hnf4g* knockout mice (*Hnf4g*$^{+/-}$) were obtained from Deltagen (San Carlos CA, USA). Briefly, *Hnf4g* knockout mice were generated by homologous recombination using ES cells derived from 129/OlaHsd mouse substrain. F1 mice were generated by breeding chimeras carrying a disrupted *Hnf4g* gene with C57BL/6 females resulting in F1 heterozygote offspring. *Hnf4g*$^{+/-}$ mice on a C57BL/6J genetic background, were

mated to obtain *Hnf4g*$^{-/-}$ mice on the same genetic background. *Hnf4g*$^{-/-}$ male mice were compared with C57Bl/6J wild-type male WT mice, matched in age and housed in the same room.

Mice were housed in groups and maintained on a 12-hour light-dark cycle with *ad libitum* access to water and diet: chow diet (CD: 5% Kcal fat - reference A03/R03, Safe-Diets) or high fat diet (60% Kcal fat - D12492, Research Diets) with 30% fructose (Sigma) in drinking water (HF-HF). Diets detail composition are described in Table 1. Mice were 2 month-old when HF-HF diet started for 6 weeks. Mice were euthanized by cervical dislocation. Experimental procedures agreed with the French ethical guidelines for animal studies and were approved by the Regional Animal Care and Use Ethic Committee Charles Darwin C2EA – 05, agreement number (#4132 – 2016021710083817 v3).

Glucose tolerance test

Glucose tolerance tests were performed after 6 weeks of HF-HF or control diets. After overnight fasting, mice received a 3.6g/kg glucose load for oral glucose tolerance tests (OGTT). Blood glucose concentrations were measured with a glucometer (Accu-checkGo, Roche). Blood samples (70µl at t0 and 10 min after glucose challenge) were collected from the tail into EDTA pre-coated microvette (Sarstedt). Plasma insulin (Alpco) and total glucagon-like peptide-1 (GLP-1) (Millipore) were measured by ELISA.

Plasma triglyceride levels after an olive oil bolus

The plasma triglyceride levels after an olive oil bolus were measured after 6 weeks of HF-HF or control diets. After overnight fasting, mice received a 200 microL olive oil load. Blood samples were collected as described in paragraph 2.2 at 0, 30, 60, 90 and 120 min after the olive oil challenge. Plasma triglyceride concentrations were measured with the kit Triglycerides FS (DiaSys).

Metabolic parameters, body composition and stool analysis

 Accepted Manuscript published as JOE-21-0092.R1. Accepted for publication: 12-Oct-2021

After 4 weeks of HF-HF or control diets, mice were housed individually in metabolic cages (Phenomaster, TSE Systems) 1 week for habituation and 1 week for measurement and were fed *ad libitum* with control or HF-HF diet. Food and water intake as well as O2 consumption, CO2 production, respiratory quotient, whole energy expenditure were automated measured. The tridimensional locomotor activity is measured by the spontaneous (voluntary) activity on the cage surface (XY axes) and in height (XZ axes). A count is register every time an infrared beam is broken in the horizontal plane or in the vertical plane. The locomotor activity was recorded for 5 consecutive days during nights and days and the mean of records was calculated. The tridimensional locomotor activity is expressed as the sum of the XY activity mean (day and night) and of the XZ activity mean (day and night) as counts in 24h / mouse. The whole body composition was analyzed with the Bruker's minispec Whole Body Composition Analyzer. This analyzer for measurement of lean tissue, fat and fluid in living mice is based on Time Domain (TD)-Nuclear magnetic resonance (NMR). Stools were daily collected and stored at -20°C. After homogenization, total and, lipid and nitrogen energy contents were ~~as~~ determined as previously described in (Layec et al., 2013).

Intestinal GLP-1 protein content

Proximal jejunum, distal ileum, and whole colon were sliced into small pieces, homogenized in ethanol/acid (100% ethanol/sterile water/12N HCl 74:25:1 v/v/v) solution (5 ml/g tissue) and incubated overnight at 4°C. Homogenates were centrifuged and supernatants were collected for total GLP-1 content measurement using ELISA kit (Millipore).

Intestinal epithelial cell isolation and protein concentration measurement

After flushing with PBS, jejunum was cut into small pieces and incubated 4h (4°C) in Cell recovery solution (BD Biosciences) containing 2% protease inhibitors (Sigma). Epithelial cells were filtered, centrifuged, and washed with PBS, to obtain epithelial cell suspension (Archer et al., 2005). Proteins were extracted from an aliquot of epithelial cells with a lysis buffer (Tris

HCl 20 mM pH 7.4, NaCl 150 mM, EDTA 5 mM, Triton 1%, DOC 0.5 %, protease and phosphatase inhibitors). Protein concentration was determined with the BCA protein assay kit (Pierce).

Triglyceride levels in epithelial cells

Lipids were extracted from an aliquot of epithelial cells with five volumes of chloroform-methanol (2:1 vol/vol), with vigorous shaking for 5 min. After centrifugation for 20 min at 1,000 *g*, the lower organic phase was collected and dried at 45°C overnight. The triglyceride levels were measured with the TG PAP 150 kit (Biomérieux).

RNA extraction and gene expression analysis

Total RNA were isolated from jejunum epithelial cells with Trizol reagent (MRC). Reverse transcription (RT) was performed with 5µg of RNA. Semi quantitative real-time PCR was performed with SYBR green (Applied) in a Stratagene system. Primer sequences are reported in Table 2.

Statistical Tests

Results are expressed as means ± SEM. Statistical analyses were performed using GraphPad Prism (GraphPad Software, La Jolla, CA). Identified outliers with the method « ROUT Q=1% » (Graphpad prism software) were removed. The significance was evaluated by 1-way ANOVA or 2-way ANOVA and followed by four Tukey's multiple comparisons tests: WT vs *Hnf4g*$^{-/-}$ on CD, WT vs *Hnf4g*$^{-/-}$ on HF-HF, WT CD vs WT HF-HF, *Hnf4g*$^{-/-}$ CD vs *Hnf4g*$^{-/-}$ HFHF. A P value <0.05 was considered statistically significant.

Results

Impact of *Hnf4g* gene invalidation on weight gain induced by a high-fat/high-fructose.

Accepted Manuscript published as JOE-21-0092.R1. Accepted for publication: 12-Oct-2021

Metabolic characteristics of *Hnf4g*$^{-/-}$ mice were compared with those of WT mice, both groups being fed *ad libitum* either with control diet or high-fat/high fructose (HF-HF) diet. The body weight gain curves were comparable between WT and *Hnf4g*$^{-/-}$ mice fed control diet. There was no weight gain after 6 weeks (99% for WT vs 94% for *Hnf4g*$^{-/-}$) (Fig. 1A). As expected, 6 weeks of HF-HF diet promoted weight gain by 35% in WT mice but surprisingly, by only 10% in *Hnf4g*$^{-/-}$ mice (Fig. 1A). We then performed a body composition analysis by NMR. On control diet, *Hnf4g*$^{-/-}$ mice showed a non-significant 1.5-fold higher fat mass than WT mice (Fig. 1B). As expected, on HF-HF diet WT mice showed a 2.4-fold increase in fat mass whereas *Hnf4g*$^{-/-}$ mice only 1.5-fold (Fig. 1B). However, on HF-HF diet, the increase in fat mass was 1.6-fold lower in *Hnf4g*$^{-/-}$ mice than in WT mice (Fig. 1B). In parallel, lean mass of *Hnf4g*$^{-/-}$ mice was similar to that of WT mice regardless the diet (data not shown). Thus *Hnf4g gene* invalidation led to a partial protection against diet-induced weight gain characterized by less fat-mass gain. In order to explain such a resistance to weight gain, we analyzed food intake, locomotor activity and energy expenditure.

Impact of high-fat/high-fructose diet on *Hnf4g*$^{-/-}$ mouse energy homeostasis

We next analyzed the energy homeostasis of WT and *Hnf4g*$^{-/-}$ mice fed control or HF-HF diets in metabolic cages after 5 weeks of diet. We showed that total calorie intake (high-fat pellets and fructose in the drinking water) normalized by mouse body weight was not affected by *Hnf4g* gene invalidation regardless the diet (Fig. 1C). The XY and XZ axis locomotor activity was next recorded. There was no significant difference between WT and *Hnf4g*$^{-/-}$ mice for their XYZ axis locomotor activity regardless the diet but HF-HF diet induced a 1.4-fold decrease in the locomotor activity regardless the mouse genotype (Fig. 1D). The calculated energy expenditure (normalized to mouse body weight) of *Hnf4g*$^{-/-}$ mice was similar to that of WT

mice fed control diet (Fig. 1E). As expected, the energy expenditure of WT fed HF-HF diet is 10% decreased compared to WT mice fed control diet (Fig. 1E). However, the energy expenditure of *Hnf4g*$^{-/-}$ mice fed control diet is similar to that of fed HF-HF diet (Fig. 1E). Thus, the WT mice weight gain, induced by HF-HF diet, is explained by an increase in fat mass, a decrease in locomotor activity and in energy expenditure. However, the partial protection to diet-induced weight gain of *Hnf4g*$^{-/-}$ mice was not due to a decrease in calorie intake, an increase in locomotor activity nor an energy expenditure. Then, we made the hypothesis that *Hnf4g* gene invalidation leads to nutrient malabsorption revealed by HF-HF diet.

Impact of *Hnf-4γ* gene invalidation on nutrient absorption

For assessment of intestinal absorption total calories were measured in feces. We showed a 25% increase in fecal calorie loss in *Hnf4g*$^{-/-}$ mice fed HF-HF diet compared to WT mice (Fig. 2A). More strikingly, this calorie loss is mainly due to a 4-fold increase of lipids in feces (Fig. 2B) whereas the protein and carbohydrate amounts were similar regardless genotypes and diets (*data not shown*). The higher calorie loss in *Hnf4g*$^{-/-}$ mice could be responsible ~~of~~ for the protection against weight gain induced by HF-HF diet. We made the hypothesis that the *Hnf4g* gene invalidation leads to a lipid malabsorption.

We measured the triglyceride level in jejunal epithelial cells and showed that in *Hnf4g*$^{-/-}$ mice fed control diet, intra-epithelial triglyceride amount is increased 2-fold (not significant) compared to WT mice. More strikingly, in WT mice fed HF-HF, the intra-epithelial triglycerides are increased 10-fold compared to that of control diet, whereas in *Hnf4g*$^{-/-}$ mice, the 2.6-fold increase is not-significant (Fig. 2C).

We then analyzed the kinetic of plasma triglyceride concentrations after an olive oil bolus, as reflect of enterocyte triglyceride secretion. The plasma triglyceride concentrations after an olive

 Accepted Manuscript published as JOE-21-0092.R1. Accepted for publication: 12-Oct-2021

oil bolus are similar in WT and *Hnf4g*$^{-/-}$ mice fed control diet. As expected under HF-HF, the concentration of plasma triglycerides in WT mice is increased 3- fold at 90min compared to that of mice on control diet whereas the concentration of plasma triglycerides in *Hnf4g*$^{-/-}$ mice remains similar to that of on control diet (Fig. 2D).

The partial protection to diet-induced weight gain of *Hnf4g*$^{-/-}$ mice could be due to an intestinal lipid malabsorption at uptake step (showed by increased lipids in feces and decreased in jejunal epithelial cells) and at secretion step (showed by plasma concentrations).

Impact of high-fat/high-fructose diet on gene expression involved in lipid absorption in *Hnf4g*$^{-/-}$ mice gut epithelium

We next analyzed gene expression of lipid membrane transporters in jejunum from *Hnf4g*$^{-/-}$ and WT mice fed control or HF-HF diet (Fig. 3A). The HF-HF diet increased the fatty acid transporter gene expression *Fabpm* and *Cd36*, regardless the mouse genotype, *Hnf4g*$^{-/-}$ or WT (Fig. 3A, upper panels). The gene expression of the fatty acid transporter *Fatp4* was reduced by 1.8-fold in *Hnf4g*$^{-/-}$ mice compared to WT mice, fed control diet and by 1.3-fold on mice fed HF-HF diet (Fig. 3A, lower left panel). The gene expression of the cholesterol transporter *Scarb1* (encoding SR-B1) was reduced in *Hnf4g*$^{-/-}$ mice compared to WT mice, regardless the diet, CD or HF-HF. However the HF-HF diet increased the Scarb1 gene expression whatever the mouse genotype, *Hnf4g*$^{-/-}$ or WT (Fig. 3A, lower right panel).

Then, we analyzed expression of genes involved in lipid storage (*Plin2*, encoding Perilipin 2 or ADRP) and secretion (*Mttp* and *ApoB*) (Fig. 3B). The HF-HF diet induced an increased gene expression of *Plin2* (2.4-fold) and of *Mttp* (1.8-fold) in WT mice but not in *Hnf4g*$^{-/-}$ mice. However, the expression of *Plin2*, *Mttp* and *apoB* is lowered in *Hnf4g*$^{-/-}$ mice fed HF-HF diet by 1.5-, 3.9- and 1.8-fold, respectively compared to WT mice fed HF-HF diet (Fig. 3B).

This decrease in gene expression of lipid transporters, lipid storage and secretion proteins could explain in part the lipids fecal calorie loss suggesting a lipid malabsorption due to lipid transfer failing toward blood circulation.

Note that gene expression of *Hnf4a* was 1.6- and 2.4-fold increase in *Hnf4g*$^{-/-}$ mice than in WT mice on control and HF-HF diets, respectively (Fig. 3C).

Impact of high-fat/high-fructose diet on *Hnf4g*$^{-/-}$ mice glucose homeostasis

The lipid malabsorption that could protect *Hnf4g*$^{-/-}$ mice against weight gain induced by an HF-HF diet, could also allow a preferential use of glucose and thus protects from a deregulation of glucose homeostasis. We challenged glucose tolerance by an OGTT and as expected, WT mice fed HF-HF present a glucose intolerance compared to WT mice fed control diet (Fig. 4A). The area under the curve (AUC) was 1.8- fold higher in WT mice fed HF-HF diet than in WT mice fed control diet (Fig. 4B). We also confirmed as previously described in Baraille & al, that *Hnf4g* gene invalidation led to improvement of glucose tolerance in mice fed control diet (Fig. 4A) (Baraille et al., 2015). Indeed, the AUC was 1.4- fold lower in *Hnf4g*$^{-/-}$ mice fed control diet than in WT mice (Fig. 4B). This feature was further exacerbated in *Hnf4g*$^{-/-}$ mice fed HF-HF diet compared to WT mice (Fig. 4A) since AUC was 1.8-fold lower in *Hnf4g*$^{-/-}$ HF-HF fed mice than in WT mice (Fig. 4A). Importantly, AUC of oral glucose tolerance test of *Hnf4g*$^{-/-}$ HF-HF fed mice was similar to that of WT control diet fed mice (Fig. 4B). As expected, fasting blood glucose and insulin were increased 1.18- and 2.74- fold respectively, in WT mice fed HF-HF compared to control diet (Fig. 4C, D) whereas fasting blood glucose and insulin remained unaffected in *Hnf4g*$^{-/-}$ mice fed HF-HF compared to control diet (Fig. 4C and D). Furthermore, the HF-HF diet induced a 3.3-fold increase of HOMA-IR in WT mice without significant effect

 Accepted Manuscript published as JOE-21-0092.R1. Accepted for publication: 12-Oct-2021

297 on HOMA-IR in *Hnf4g*$^{-/-}$ mice (Fig. 4E). These results indicate that *Hnf4g* gene invalidation
298 protects mice against glucose intolerance induced by the HF-HF diet.
299
300 **Impact of high-fat/high-fructose diet on *Hnf4g*$^{-/-}$ mice GLP-1 intestinal homeostasis**
301
302 We then measured the total plasma GLP-1 concentration 10 min after a glucose challenge. As
303 previously described in Baraille & al, we confirmed that plasma total GLP-1 concentration was
304 3.3-fold increase in *Hnf4g*$^{-/-}$ than in WT mice fed control diet, (Fig. 5A) (Baraille et al., 2015).
305 Although the HF-HF diet induced a 3-fold increase in plasma total GLP-1 concentration in WT
306 mice and a 1.4-fold non-significant increase in *Hnf4g*$^{-/-}$ mice, the plasma total GLP-1
307 concentration in *Hnf4g*$^{-/-}$ mice fed HF-HF remained 1.53 fold higher than in WT mice fed HF-
308 HF (Fig. 5A). We next measured GLP-1 content in mouse jejunum and we showed that GLP-1
309 content in jejunum of *Hnf4g*$^{-/-}$ mice is 2- and 1.7-fold increase in control and HF-HF diet,
310 respectively (Fig. 5B). In jejunum, the level of *Gcg* mRNA, encoding proglucagon, is increased
311 by HF-HF diet 1.95- and 1.6-fold in WT and *Hnf4g*$^{-/-}$ mice, respectively (Fig. 5C). These results
312 showed that the *Hnf4g* gene invalidation leads to an increase in GLP-1 jejunum content that
313 could explain the increase in plasma GLP-1 in response to glucose challenge in mice fed control
314 and HF-HF diet.
315
316 **Discussion**
317
318 Our results demonstrate that the gene invalidation of the nuclear receptor HNF-4γ induces a
319 protection against the weight gain induced by a high-fat/high-fructose diet. The weight gain
320 protection is mainly due to intestinal lipid malabsorption leading to a calorie loss in feces.
321 *Hnf4g*$^{-/-}$ mice were also protected against glucose intolerance induced by the HF-HF diet. An

322 increase in jejunal GLP-1 content could participate to this protection *via* a possible incretin
323 effect.
324 Mice invalidated for *Hnf4g* gene were reported to present a lower food intake, associated with
325 lower night energy expenditure, than wild type mice (Gerdin et al., 2006). Our previous results
326 did not show difference in food intake in *Hnf4g*$^{-/-}$ and *WT* mice fed control diet but a strong
327 improvement of glucose tolerance of *Hnf4g*$^{-/-}$ mice (Baraille et al., 2015), suggesting that HNF-
328 4γ could be involved in susceptibility to type 2 diabetes. In order to generate rapid glucose
329 intolerance and insulin resistance, we challenged mice with a high fat and high fructose diet.
330 This long term diet (16 weeks) is widely used to induce NASH but a glucose intolerance along
331 with insulin resistance appear earlier after 4 weeks of diet along with weight gain (Charlton et
332 al., 2011; Dissard et al., 2013; Tsuchiya et al., 2013). As expected we observed in WT mice fed
333 HF-HF a weight gain from one week and a glucose intolerance at 6 weeks that are mainly due
334 to an increase in fat mass and a decrease in locomotor activity and in energy expenditure. One
335 of the most striking effect of *Hnf4g* gene invalidation is a weight gain and a glucose intolerance
336 protection against HF-HF diet. We could expect an increase in energy expenditure or in
337 locomotor activity to explain this protection. However, energy homeostasis analysis in
338 metabolic cages does not show differences between WT and *Hnf4g*$^{-/-}$ mice fed HF-HF. We
339 hypothesized that *Hnf4g* gene invalidation induces a loss of ingested calories and we showed
340 increased calories in feces. We made the hypothesis of a lipid failing absorption revealed by
341 the HF-HF diet challenge.
342 Enterocytes ensure the absorption of dietary lipids to the organism through complex processes
343 that can be summarized into three major steps: uptake, storage and/or secretion (Williams,
344 2008). The increase lipid content in feces, the decrease in intra-epithelium triglyceride content
345 and the decrease of plasma triglyceride concentration after an olive oil bolus indicate that *Hnf4g*
346 gene invalidation in HF-HF diet fed mice leads to a lipid malabsorption at the three major steps

 Accepted Manuscript published as JOE-21-0092.R1. Accepted for publication: 12-Oct-2021

uptake, storage and secretion. We expected a down-regulation of lipid transporters gene expression in *Hnf4g*$^{-/-}$ mice fed HF-HF. Although HF-HF diet induces an increase in gene expression of fatty acid transporters, such as the *Cd36* and *Fabpm* in jejunum of both *Hnf4g*$^{-/-}$ and *WT* mice, *Hnf4g* gene invalidation impacts the gene expression of *Fatp4* and *Scarb1* regardless the diet.

We could hypothesize that gene expression of lipid transporters *Cd36* and *Fabpm* is up-regulated to compensate a lipid malabsorption in *Hnf4g*$^{-/-}$ mice fed HF-HF. Although there is a gene overexpression of these transporters, we cannot exclude a translational down regulation of these transporters or a membrane mislocalization, both could participate in lipid malabsorption.

Although the role of FATP4 as a transporter for fatty acid uptake remains unclear, it has been shown that intestinal FATP4 is exclusively found intracellular instead of on the plasma membrane. FATP4 plays a role in fatty acid uptake through its intrinsic intracellular enzymatic activity, through a process known as “vectorial acylation”, i.e., the obligatory step of acyl-CoA formation for fatty acid transport across the plasma membrane, from intestinal lumen toward enterocytes (Digel et al., 2011; Milger et al., 2006). Thereby, a 25% decrease in *Fatp4* expression could participate to lipid malabsorption in *Hnf4g*$^{-/-}$ mice fed HF-HF.

The scavenger receptor is known for its function as a cholesterol transporter SR-B1, however its role in cholesterol and lipid metabolism remains unclear in intestine. It has been shown *in vitro* that addition of lipid micelles triggers SR-B1 lipid sensing and a signaling cascade leading to ApoB translocation from the apical membrane to the secretory basolateral domains (Beaslas et al., 2009; Saddar et al., 2013). Some reports show that SR-B1 plays an important role in intestinal chylomicron production (Bura et al., 2013; Hayashi et al., 2011). Thus, through an indirect effect, the decrease in *Scarb1* gene expression prevents the lipid transfer in *Hnf4g*$^{-/-}$ mice fed HF-HF.

372 The chylomicron production loss is amplified by the decrease in gene expression of *Mttp* and
373 *ApoB* that are necessary to the production of the lipoprotein particle.
374 A defect in biliary acid metabolism could also account for lipid malabsorption. When the
375 entero-hepatic biliary acid cycle leading to micelle formation is deficient, dietary lipids are not
376 properly embedded with micelles, precluding adequate absorption by enterocytes (Nordskog et
377 al., 2001). A down regulation of pancreatic lipase expression, enzyme responsible of dietary
378 lipid hydrolysis before micelle embedding, could also be questioned (Alkaade and Vareedayah,
379 2017).
380 In our previous work, we demonstrated that HNF-4γ plays a critical role in glucose homeostasis
381 and that HNF-4γ loss leads to an improvement of glucose tolerance through a rise of GLP-1
382 incretin effect (Baraille et al., 2015). Here we show that the glucose tolerance improvement is
383 maintained in *Hnf4g*$^{-/-}$ mice despite HF-HF feeding, in such a way that *Hnf4g* gene invalidation
384 leads to a protection against the dietary glucose intolerance. The HOMA-IR was significantly
385 increased only in WT mice fed HF-HF diet, indicating a possible protection of *Hnf4g*
386 invalidation against insulin resistance too. Accordingly, the jejunum GLP-1 content is increased
387 in *Hnf4g*$^{-/-}$ mice fed HF-HF. The expression of *Gcg* gene, encoding GLP-1 in intestine, are
388 increased in *Hnf4g*$^{-/-}$ mice fed control diet and are maintained in *Hnf4g*$^{-/-}$ mice fed HF-HF. The
389 loss of HNF-4γ improves the GLP-1 producing cell homeostasis, leading to a protection against
390 a diet-induced deregulated glucose homeostasis.
391 The effects of *Hnf4g* gene invalidation are of two types. The first is an invalidation effect seen
392 regardless of diet, CD or HF-HF. This is the case with glucose tolerance and plasma and
393 intraepithelial concentrations of GLP-1 as well as expression of *Hnf4a*. The second is an effect
394 of invalidation revealed by the HF-HF diet. This is the case with the amount of calories and
395 lipids found in the feces as well as plasma triglyceride concentrations, thus revealing lipid
396 malabsorption. In addition, the expression of genes involved in the uptake, storage and secretion

 Accepted Manuscript published as JOE-21-0092.R1. Accepted for publication: 12-Oct-2021

of lipids such as *Fatp4*, *Scarb1*, *Plin2*, *Mttp*, and *ApoB* is also impacted by the invalidation of *Hnf4g* with the HF-HF diet. It should be noted that the expression of the *Fatp4* transporter is also impacted under the CD diet.

In absence of HNF-4γ, there is an overexpression of HNF-4α regardless the diet. It is difficult to assert that the observed effects were the direct consequence of HNF-4γ loss or resulted indirectly from HNF-4α increment in *Hnf4g*$^{-/-}$ mouse intestine. However, we could hypothesized that HNF-4α is able to compensate the loss of HNF-4γ for intestinal lipid absorption under control diet but that is overtaken under HF-HF diet. HNF-4α and HNF-4γ are encoded by two different genes but share high homology in their DNA and ligand binding domains (Drewes et al., 1996; Taraviras et al., 2000). Indeed, it has been recently shown that HNF-4α and HNF-4γ share almost all their binding sites on chromatin (Chen et al., 2019) and regulate the expression of genes involved in fatty-acid oxydation (Chen et al., 2020). However, these two transcription factors have a different spatial distribution along the crypt-villus axis, HNF-4α being expressed along the crypt to villus axis and HNF-4γ being restricted to the villus (Sauvaget et al., 2002). Furthermore, 9 isoforms of HNF-4α raised from differential splicing and from 2 different promoters have been described (Torres-Padilla et al., 2001). These isoforms can have opposite roles in colitis and colitis associated colon cancer (Chellappa et al., 2016). These observations show that the two forms of HNF-4, HNF-4α and HNF-4γ play some specific roles but we cannot exclude redundancy for others roles, the balance between the expression of HNF-4α and HNF-4γ being finely regulated to maintain gut homeostasis.

In recent report, it has been shown that *Hnf4a* and *Hnf4g* are redundantly required to drive intestinal differentiation (Chen et al., 2019). Genes that exhibit a direct binding of HNF-4α or γ are involved in lipid metabolim (Chen et al., 2019). However, an indirect regulation is also possible since it HNF-4 α and γ function maintain also active enhancer chromatin (Chen et al.,

2019). However, the transcriptome analysis reveals that *Hnf4g* invalidation alters specifically the expression of 89 genes in intestine. Thus we cannot exclude a direct binding of HNF-4g on genes involved in lipid metabolism such as Fatp4 and Scarb1, the Hnf4a expression being repressed by the antisense transcript of Hnf4a previously described (Lindeboom et al., 2018). In our previous article, we showed that proglucagon (Gcg) gene transcription was not directly activated or repressed by HNF-4a or HNF-4g but rather the expression of Foxa1, Foxa2, and Isl1 was enhanced, suggesting that modifications of the transcription factor network favored the GLP-1–secreting cell lineage (Baraille et al., 2015).

In conclusion, we demonstrated that loss of HNF-4γ in mice prevents obesity and glucose intolerance induced by HF-HF diet. The protection against metabolic deleterious effects of HF-HF diet could be due to intestinal lipid malabsorption and glucose homeostasis improvement. Interestingly in human, *HNF4G* was identified as an obesity-associated locus in a meta-analysis of GWAS study (Berndt et al., 2013) and could also be associated with pediatric obesity (Selvanayagam et al., 2018).

Acknowledgments

We thank C Ayassamy (Centre d'Exploration Fonctionnelle –UMRS 1138) for mouse care, C Amorin (Centre de génotypage et de biochimie – UMRS 1138) for mouse genotyping and A Lacombe (Preclin – IHU ICAN) for metabolic cage experiments.

Author contribution statement

S.A., C.O., E.G.-I., L.L.G., N.K., H.S. and A.R. designed experiments, acquired and analyzed data. S.A., H.S., F.A., K.C., P.S., A.L. and A.R. contributed to data interpretation and to the discussion. S.A., H.S., P.S., A.L. and A.R. wrote the manuscript. P.S. and A.R. reviewed and edited manuscript. A.R. is the guarantor of this work and, as such, had full access to all data in

 Accepted Manuscript published as JOE-21-0092.R1. Accepted for publication: 12-Oct-2021

446 the study and takes responsibility for the integrity of the data and the accuracy of the data
447 analysis.
448
449 **Funding**
450 This work was supported by INSERM, France, and Pierre & Marie Curie University (UPMC),
451 Paris, France. S.A. and L.L.G. were recipient of a doctoral fellowship from Sorbonne
452 Université. E.G.I. was recipient of an internship fellowship from University of Navarra and
453 Caixa Bank (Spain).
454
455 **Declaration of interest**
456 No potential conflicts of interest relevant to this article were reported.
457
458 **Prior presentation.** Parts of these data were presented at 51st annual meeting of the European
459 Association for the Study of Diabetes (Diabetologia, 58 S28, 2015).
460
461

References

Adeli, K., and Lewis, G.F. (2008). Intestinal lipoprotein overproduction in insulin-resistant states. Curr Opin Lipidol *19*, 221-228.

Alkaade, S., and Vareedayah, A.A. (2017). A primer on exocrine pancreatic insufficiency, fat malabsorption, and fatty acid abnormalities. Am J Manag Care *23*, S203-S209.

Archer, A., Sauvaget, D., Chauffeton, V., Bouchet, P.E., Chambaz, J., Pincon-Raymond, M., Cardot, P., Ribeiro, A., and Lacasa, M. (2005). Intestinal apolipoprotein A-IV gene transcription is controlled by two hormone-responsive elements: a role for hepatic nuclear factor-4 isoforms. Mol Endocrinol *19*, 2320-2334.

Bansal, S., Buring, J.E., Rifai, N., Mora, S., Sacks, F.M., and Ridker, P.M. (2007). Fasting compared with nonfasting triglycerides and risk of cardiovascular events in women. JAMA *298*, 309-316.

Baraille, F., Ayari, S., Carriere, V., Osinski, C., Garbin, K., Blondeau, B., Guillemain, G., Serradas, P., Rousset, M., Lacasa, M., et al. (2015). Glucose Tolerance Is Improved in Mice Invalidated for the Nuclear Receptor HNF-4gamma: A Critical Role for Enteroendocrine Cell Lineage. Diabetes *64*, 2744-2756.

Battle, M.A., Konopka, G., Parviz, F., Gaggl, A.L., Yang, C., Sladek, F.M., and Duncan, S.A. (2006). Hepatocyte nuclear factor 4alpha orchestrates expression of cell adhesion proteins during the epithelial transformation of the developing liver. Proc Natl Acad Sci U S A *103*, 8419-8424.

Beaslas, O., Cueille, C., Delers, F., Chateau, D., Chambaz, J., Rousset, M., and Carriere, V. (2009). Sensing of dietary lipids by enterocytes: a new role for SR-BI/CLA-1. PLoS One *4*, e4278.

Benoit, G., Cooney, A., Giguere, V., Ingraham, H., Lazar, M., Muscat, G., Perlmann, T., Renaud, J.P., Schwabe, J., Sladek, F., et al. (2006). International Union of Pharmacology. LXVI. Orphan nuclear receptors. Pharmacol Rev *58*, 798-836.

Berndt, S.I., Gustafsson, S., Magi, R., Ganna, A., Wheeler, E., Feitosa, M.F., Justice, A.E., Monda, K.L., Croteau-Chonka, D.C., Day, F.R., et al. (2013). Genome-wide meta-analysis identifies 11 new loci for anthropometric traits and provides insights into genetic architecture. Nat Genet *45*, 501-512.

Accepted Manuscript published as JOE-21-0092.R1. Accepted for publication: 12-Oct-2021

493 Bookout, A.L., Jeong, Y., Downes, M., Yu, R.T., Evans, R.M., and Mangelsdorf, D.J. (2006).
494 Anatomical profiling of nuclear receptor expression reveals a hierarchical transcriptional
495 network. Cell *126*, 789-799.

496 Bura, K.S., Lord, C., Marshall, S., McDaniel, A., Thomas, G., Warrier, M., Zhang, J., Davis,
497 M.A., Sawyer, J.K., Shah, R., et al. (2013). Intestinal SR-BI does not impact cholesterol
498 absorption or transintestinal cholesterol efflux in mice. J Lipid Res *54*, 1567-1577.

499 Cattin, A.L., Le Beyec, J., Barreau, F., Saint-Just, S., Houllier, A., Gonzalez, F.J., Robine, S.,
500 Pincon-Raymond, M., Cardot, P., Lacasa, M., et al. (2009). Hepatocyte nuclear factor
501 4alpha, a key factor for homeostasis, cell architecture, and barrier function of the adult
502 intestinal epithelium. Mol Cell Biol *29*, 6294-6308.

503 Charlton, M., Krishnan, A., Viker, K., Sanderson, S., Cazanave, S., McConico, A., Masuoko,
504 H., and Gores, G. (2011). Fast food diet mouse: novel small animal model of NASH with
505 ballooning, progressive fibrosis, and high physiological fidelity to the human condition.
506 Am J Physiol Gastrointest Liver Physiol *301*, G825-834.

507 Chellappa, K., Deol, P., Evans, J.R., Vuong, L.M., Chen, G., Briancon, N., Bolotin, E., Lytle,
508 C., Nair, M.G., and Sladek, F.M. (2016). Opposing roles of nuclear receptor HNF4alpha
509 isoforms in colitis and colitis-associated colon cancer. Elife *5*.

510 Chen, L., Toke, N.H., Luo, S., Vasoya, R.P., Fullem, R.L., Parthasarathy, A., Perekatt, A.O.,
511 and Verzi, M.P. (2019). A reinforcing HNF4-SMAD4 feed-forward module stabilizes
512 enterocyte identity. Nat Genet *51*, 777-785.

513 Chen, L., Vasoya, R.P., Toke, N.H., Parthasarathy, A., Luo, S., Chiles, E., Flores, J., Gao, N.,
514 Bonder, E.M., Su, X., et al. (2020). HNF4 Regulates Fatty Acid Oxidation and Is Required
515 for Renewal of Intestinal Stem Cells in Mice. Gastroenterology *158*, 985-999 e989.

516 Davidson, N.O., and Shelness, G.S. (2000). APOLIPOPROTEIN B: mRNA editing, lipoprotein
517 assembly, and presecretory degradation. Annu Rev Nutr *20*, 169-193.

518 Digel, M., Staffer, S., Ehehalt, F., Stremmel, W., Ehehalt, R., and Fullekrug, J. (2011). FATP4
519 contributes as an enzyme to the basal and insulin-mediated fatty acid uptake of C(2)C(1)(2)
520 muscle cells. Am J Physiol Endocrinol Metab *301*, E785-796.

521 Dissard, R., Klein, J., Caubet, C., Breuil, B., Siwy, J., Hoffman, J., Sicard, L., Ducasse, L.,
522 Rascalou, S., Payre, B., et al. (2013). Long term metabolic syndrome induced by a high fat
523 high fructose diet leads to minimal renal injury in C57BL/6 mice. PLoS One *8*, e76703.

524 Drewes, T., Senkel, S., Holewa, B., and Ryffel, G.U. (1996). Human hepatocyte nuclear factor
525 4 isoforms are encoded by distinct and differentially expressed genes. Mol Cell Biol *16*,
526 925-931.

527 Duez, H., Lamarche, B., Uffelman, K.D., Valero, R., Cohn, J.S., and Lewis, G.F. (2006).
528 Hyperinsulinemia is associated with increased production rate of intestinal apolipoprotein
529 B-48-containing lipoproteins in humans. Arterioscler Thromb Vasc Biol *26*, 1357-1363.

530 Duez, H., Pavlic, M., and Lewis, G.F. (2008). Mechanism of intestinal lipoprotein
531 overproduction in insulin resistant humans. Atheroscler Suppl *9*, 33-38.

532 Frochot, V., Alqub, M., Cattin, A.L., Carriere, V., Houllier, A., Baraille, F., Barbot, L., Saint-
533 Just, S., Ribeiro, A., Lacasa, M., et al. (2012). The transcription factor HNF-4alpha: a key
534 factor of the intestinal uptake of fatty acids in mouse. Am J Physiol Gastrointest Liver
535 Physiol *302*, G1253-1263.

536 Gerdin, A.K., Surve, V.V., Jonsson, M., Bjursell, M., Bjorkman, M., Edenro, A., Schuelke, M.,
537 Saad, A., Bjurstrom, S., Lundgren, E.J., et al. (2006). Phenotypic screening of hepatocyte
538 nuclear factor (HNF) 4-gamma receptor knockout mice. Biochem Biophys Res Commun
539 *349*, 825-832.

540 Gimeno, R.E., Hirsch, D.J., Punreddy, S., Sun, Y., Ortegon, A.M., Wu, H., Daniels, T., Stricker-
541 Krongrad, A., Lodish, H.F., and Stahl, A. (2003). Targeted deletion of fatty acid transport
542 protein-4 results in early embryonic lethality. J Biol Chem *278*, 49512-49516.

543 Haidari, M., Leung, N., Mahbub, F., Uffelman, K.D., Kohen-Avramoglu, R., Lewis, G.F., and
544 Adeli, K. (2002). Fasting and postprandial overproduction of intestinally derived
545 lipoproteins in an animal model of insulin resistance. Evidence that chronic fructose
546 feeding in the hamster is accompanied by enhanced intestinal de novo lipogenesis and
547 ApoB48-containing lipoprotein overproduction. J Biol Chem *277*, 31646-31655.

548 Hayashi, A.A., Webb, J., Choi, J., Baker, C., Lino, M., Trigatti, B., Trajcevski, K.E., Hawke,
549 T.J., and Adeli, K. (2011). Intestinal SR-BI is upregulated in insulin-resistant states and is
550 associated with overproduction of intestinal apoB48-containing lipoproteins. Am J Physiol
551 Gastrointest Liver Physiol *301*, G326-337.

552 Hsieh, J., Hayashi, A.A., Webb, J., and Adeli, K. (2008). Postprandial dyslipidemia in insulin
553 resistance: mechanisms and role of intestinal insulin sensitivity. Atheroscler Suppl *9*, 7-13.

 Accepted Manuscript published as JOE-21-0092.R1. Accepted for publication: 12-Oct-2021

554 Hwang-Verslues, W.W., and Sladek, F.M. (2010). HNF4alpha--role in drug metabolism and
555 potential drug target? Curr Opin Pharmacol *10*, 698-705.

556 Iqbal, J., and Hussain, M.M. (2009). Intestinal lipid absorption. Am J Physiol Endocrinol Metab
557 *296*, E1183-1194.

558 Layec, S., Beyer, L., Corcos, O., Alves, A., Dray, X., Amiot, A., Stefanescu, C., Coffin, B.,
559 Bretagnol, F., Bouhnik, Y., et al. (2013). Increased intestinal absorption by segmental
560 reversal of the small bowel in adult patients with short-bowel syndrome: a case-control
561 study. Am J Clin Nutr *97*, 100-108.

562 Levy, E., Sinnett, D., Thibault, L., Nguyen, T.D., Delvin, E., and Menard, D. (1996). Insulin
563 modulation of newly synthesized apolipoproteins B-100 and B-48 in human fetal intestine:
564 gene expression and mRNA editing are not involved. FEBS Lett *393*, 253-258.

565 Lewis, G.F., Uffelman, K., Naples, M., Szeto, L., Haidari, M., and Adeli, K. (2005). Intestinal
566 lipoprotein overproduction, a newly recognized component of insulin resistance, is
567 ameliorated by the insulin sensitizer rosiglitazone: studies in the fructose-fed Syrian golden
568 hamster. Endocrinology *146*, 247-255.

569 Li, X., Udager, A.M., Hu, C., Qiao, X.T., Richards, N., and Gumucio, D.L. (2009). Dynamic
570 patterning at the pylorus: formation of an epithelial intestine-stomach boundary in late fetal
571 life. Dev Dyn *238*, 3205-3217.

572 Lindeboom, R.G., van Voorthuijsen, L., Oost, K.C., Rodriguez-Colman, M.J., Luna-Velez,
573 M.V., Furlan, C., Baraille, F., Jansen, P.W., Ribeiro, A., Burgering, B.M., et al. (2018).
574 Integrative multi-omics analysis of intestinal organoid differentiation. Mol Syst Biol *14*,
575 e8227.

576 Milger, K., Herrmann, T., Becker, C., Gotthardt, D., Zickwolf, J., Ehehalt, R., Watkins, P.A.,
577 Stremmel, W., and Fullekrug, J. (2006). Cellular uptake of fatty acids driven by the ER-
578 localized acyl-CoA synthetase FATP4. J Cell Sci *119*, 4678-4688.

579 Montenegro-Miranda, P.S., van der Meer, J.H.M., Jones, C., Meisner, S., Vermeulen, J.L.M.,
580 Koster, J., Wildenberg, M.E., Heijmans, J., Boudreau, F., Ribeiro, A., et al. (2020). A Novel
581 Organoid Model of Damage and Repair Identifies HNF4alpha as a Critical Regulator of
582 Intestinal Epithelial Regeneration. Cell Mol Gastroenterol Hepatol *10*, 209-223.

583 Nogueira, J.P., Maraninchi, M., Beliard, S., Padilla, N., Duvillard, L., Mancini, J., Nicolay, A.,
584 Xiao, C., Vialettes, B., Lewis, G.F., et al. (2012). Absence of acute inhibitory effect of

585 insulin on chylomicron production in type 2 diabetes. Arterioscler Thromb Vasc Biol *32*,
586 1039-1044.

587 Nordestgaard, B.G., Benn, M., Schnohr, P., and Tybjaerg-Hansen, A. (2007). Nonfasting
588 triglycerides and risk of myocardial infarction, ischemic heart disease, and death in men
589 and women. JAMA *298*, 299-308.

590 Nordskog, B.K., Phan, C.T., Nutting, D.F., and Tso, P. (2001). An examination of the factors
591 affecting intestinal lymphatic transport of dietary lipids. Adv Drug Deliv Rev *50*, 21-44.

592 Plengvidhya, N., Antonellis, A., Wogan, L.T., Poleev, A., Borgschulze, M., Warram, J.H.,
593 Ryffel, G.U., Krolewski, A.S., and Doria, A. (1999). Hepatocyte nuclear factor-4gamma:
594 cDNA sequence, gene organization, and mutation screening in early-onset autosomal-
595 dominant type 2 diabetes. Diabetes *48*, 2099-2102.

596 Ribeiro, A., Archer, A., Le Beyec, J., Cattin, A.-L., Saint-Just, S., Pinçon-Raymond, M.,
597 Chambaz, J., Lacasa, M., and Cardot, P. (2007). Hepatic Nuclear Factor-4, a key
598 transcription factor at the crossroads between architecture and function of epithelia. Recent
599 Patents on Endocrine, Metabolic & Immune Drug Discovery *1*, 176-181

600 Robertson, M.D., Parkes, M., Warren, B.F., Ferguson, D.J., Jackson, K.G., Jewell, D.P., and
601 Frayn, K.N. (2003). Mobilisation of enterocyte fat stores by oral glucose in humans. Gut
602 *52*, 834-839.

603 Saandi, T., Baraille, F., Derbal-Wolfrom, L., Cattin, A.L., Benahmed, F., Martin, E., Cardot,
604 P., Duclos, B., Ribeiro, A., Freund, J.N., et al. (2013). Regulation of the tumor suppressor
605 homeogene Cdx2 by HNF4alpha in intestinal cancer. Oncogene *32*, 3782-3788.

606 Saddar, S., Carriere, V., Lee, W.R., Tanigaki, K., Yuhanna, I.S., Parathath, S., Morel, E.,
607 Warrier, M., Sawyer, J.K., Gerard, R.D., et al. (2013). Scavenger receptor class B type I is
608 a plasma membrane cholesterol sensor. Circ Res *112*, 140-151.

609 Sasaki, S., Urabe, M., Maeda, T., Suzuki, J., Irie, R., Suzuki, M., Tomaru, Y., Sakaguchi, M.,
610 Gonzalez, F.J., and Inoue, Y. (2018). Induction of Hepatic Metabolic Functions by a Novel
611 Variant of Hepatocyte Nuclear Factor 4gamma. Mol Cell Biol *38*.

612 Sauvaget, D., Chauffeton, V., Citadelle, D., Chatelet, F.P., Cywiner-Golenzer, C., Chambaz, J.,
613 Pincon-Raymond, M., Cardot, P., Le Beyec, J., and Ribeiro, A. (2002). Restriction of
614 apolipoprotein A-IV gene expression to the intestine villus depends on a hormone-

 Accepted Manuscript published as JOE-21-0092.R1. Accepted for publication: 12-Oct-2021

615 responsive element and parallels differential expression of the hepatic nuclear factor 4alpha
616 and gamma isoforms. J Biol Chem *277*, 34540-34548.

617 Selvanayagam, T., Walker, S., Gazzellone, M.J., Kellam, B., Cytrynbaum, C., Stavropoulos,
618 D.J., Li, P., Birken, C.S., Hamilton, J., Weksberg, R., et al. (2018). Genome-wide copy
619 number variation analysis identifies novel candidate loci associated with pediatric obesity.
620 Eur J Hum Genet *26*, 1588-1596.

621 Shikany, J.M., and White, G.L., Jr. (2000). Dietary guidelines for chronic disease prevention.
622 South Med J *93*, 1138-1151.

623 Stahel, P., Xiao, C., Nahmias, A., and Lewis, G.F. (2020). Role of the Gut in Diabetic
624 Dyslipidemia. Front Endocrinol (Lausanne) *11*, 116.

625 Stahl, A., Hirsch, D.J., Gimeno, R.E., Punreddy, S., Ge, P., Watson, N., Patel, S., Kotler, M.,
626 Raimondi, A., Tartaglia, L.A., et al. (1999). Identification of the major intestinal fatty acid
627 transport protein. Mol Cell *4*, 299-308.

628 Taraviras, S., Mantamadiotis, T., Dong-Si, T., Mincheva, A., Lichter, P., Drewes, T., Ryffel,
629 G.U., Monaghan, A.P., and Schutz, G. (2000). Primary structure, chromosomal mapping,
630 expression and transcriptional activity of murine hepatocyte nuclear factor 4gamma.
631 Biochim Biophys Acta *1490*, 21-32.

632 Torres-Padilla, M.E., Fougere-Deschatrette, C., and Weiss, M.C. (2001). Expression of
633 HNF4alpha isoforms in mouse liver development is regulated by sequential promoter usage
634 and constitutive 3' end splicing. Mech Dev *109*, 183-193.

635 Tsuchiya, H., Ebata, Y., Sakabe, T., Hama, S., Kogure, K., and Shiota, G. (2013). High-fat,
636 high-fructose diet induces hepatic iron overload via a hepcidin-independent mechanism
637 prior to the onset of liver steatosis and insulin resistance in mice. Metabolism *62*, 62-69.

638 Vine, D.F., Takechi, R., Russell, J.C., and Proctor, S.D. (2007). Impaired postprandial
639 apolipoprotein-B48 metabolism in the obese, insulin-resistant JCR:LA-cp rat: increased
640 atherogenicity for the metabolic syndrome. Atherosclerosis *190*, 282-290.

641 Williams, K.J. (2008). Molecular processes that handle -- and mishandle -- dietary lipids. J Clin
642 Invest *118*, 3247-3259.

643

Figure legends

Figure 1: Impact of high fat-high fructose diet on energy homeostasis in *Hnf4g*$^{-/-}$ and WT mice. (A) Body weight of mice fed control diet or HF-HF diet during 6 weeks. Results were from 5 independent experiments with $12 \leq n \leq 36$ for each condition. **(B)** Body fat mass evaluated by TD-MNR at 5 weeks of diet. **(C)** Food intake is the sum of pellet quantity and drinking water volume recorded for 5 consecutive days in metabolic cages and is expressed in kcal/day/Kg mouse. Control diet = 3.2kcal/g; High-fat diet = 5.24kcal/g; Fructose 30% = 1.2kcal/mL. **(D)** The locomotor activity is the sum of XY and XZ mean locomotor activity from 5 consecutive nights and days. **(E)** The energy expenditure, measured by indirect calorimetry, is the mean of the energy expenditure from 5 consecutive nights and days. Results (B-E) were from 2 independent experiments with n= 5 to 6 mice per group. **** $p < 0.0001$; ** $p < 0.01$; * $p < 0.05$; ns not significant.

Figure 2: Impact of high fat-high fructose diet on intestinal nutrient absorption in *Hnf4g*$^{-/-}$ and WT mice. (A) Total fecal calories were determined by bomb calorimetry in daily collected feces from 3 to 5 consecutive days. Results are the mean of 4 independent measures during 2 experiments (n = 5 or 6 animals in each condition). **(B)** The lipid content into feces from *Hnf4g*$^{-/-}$ and WT mice were measured Results are the mean of 3 independent measures during 2 experiments (n = 5 or 6 animals in each condition). **(C)** The amount of triglycerides stored in epithelial cells were quantified in isolated epithelial cells. **(D)** Plasma triglyceride concentrations were measured at 30, 60, 90 and 120 min after a 200 microL olive oil bolus (T0 is indicated by an arrow). n= 4 or 5 animals per condition. *** $p < 0.001$; ** $p < 0.01$; * $p < 0.05$; ns not significant.

 Accepted Manuscript published as JOE-21-0092.R1. Accepted for publication: 12-Oct-2021

669 **Figure 3: Impact of high fat-high fructose diet on jejunal expression of genes involved in**
670 **lipid uptake, storage and secretion in *Hnf4g*$^{-/-}$ and WT mice.** Quantitative RT-PCRs for gene
671 expression of **(A)** fatty acid and cholesterol membrane transporters, **(B)** genes involved in
672 storage and secretion of chylomicrons, (C) *Hnf4a* in jejunum of *Hnf4g*$^{-/-}$ and WT mice fed
673 control diet or HF-HF diet. The mRNA levels were normalized by cyclophilin mRNA level.
674 Results were mean of 2 to 6 independent experiments with n= 4 to 12 mice per group. **** p
675 < 0.0001; *** $p < 0.001$; ** $p < 0.01$; * $p < 0.05$; ns not significant.
676 **Figure 4: Impact of high fat-high fructose diet on the glucose homeostasis in *Hnf4g*$^{-/-}$ and**
677 **WT mice.** (A) Oral glucose tolerance test (OGTT, 3.6g glucose/kg) after 15h fasting. **(B)** Area
678 under the curve of the OGTT. **(C)** Fasted blood glucose. Results (A-C) were mean of 6
679 independent experiments with n= 5 to 7 mice per group. **(D)** Fasted blood insulin. **(E)** The
680 HOMA-IR was calculated from blood glucose and insulin values in (C) and (D) as follow:
681 [fasted blood glucose (mg/dL)] x [fasted blood insulin (mU/L)] / 405. Results (D-E) were mean
682 of 3 independent experiments with n= 3 to 10 mice per group. *** $p < 0.001$; ** $p < 0.01$; * p
683 < 0.05; ns not significant.
684
685 **Figure 5: Impact of high fat-high fructose diet on the intestinal GLP-1 homeostasis in**
686 ***Hnf4g*$^{-/-}$ and WT mice.** (A) Total plasma total GLP-1 10 min after glucose bolus. Results were
687 mean of 4 independent experiments. **(B)** Total GLP-1 content in jejunum. Results were mean
688 of 2 independent experiments. **(C)** Quantitative RT-PCRs for Gcg gene expression. The mRNA
689 levels were normalized by cyclophilin mRNA level. Results were mean of 4 independent
690 experiments. *** $p < 0.001$; ** $p < 0.01$; * $p < 0.05$; ns not significant
691
692

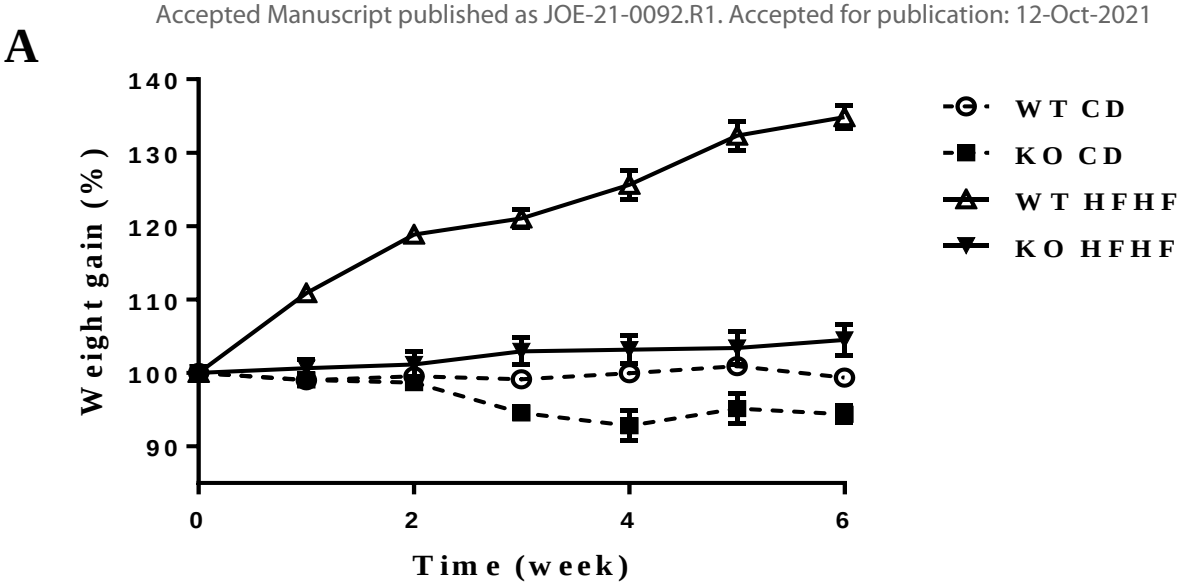

multiple comparison test	1 week	2 week	3 week	4 week	5 week	6 week
WT CD vs KO CD	ns	ns	ns	ns	*	ns
WT HFHF vs KO HFHF	ns	**	**	**	***	****
WT CD vs WT HF-HF	ns	**	***	***	***	****
KO CD vs KO HF-HF	ns	ns	ns	ns	ns	ns

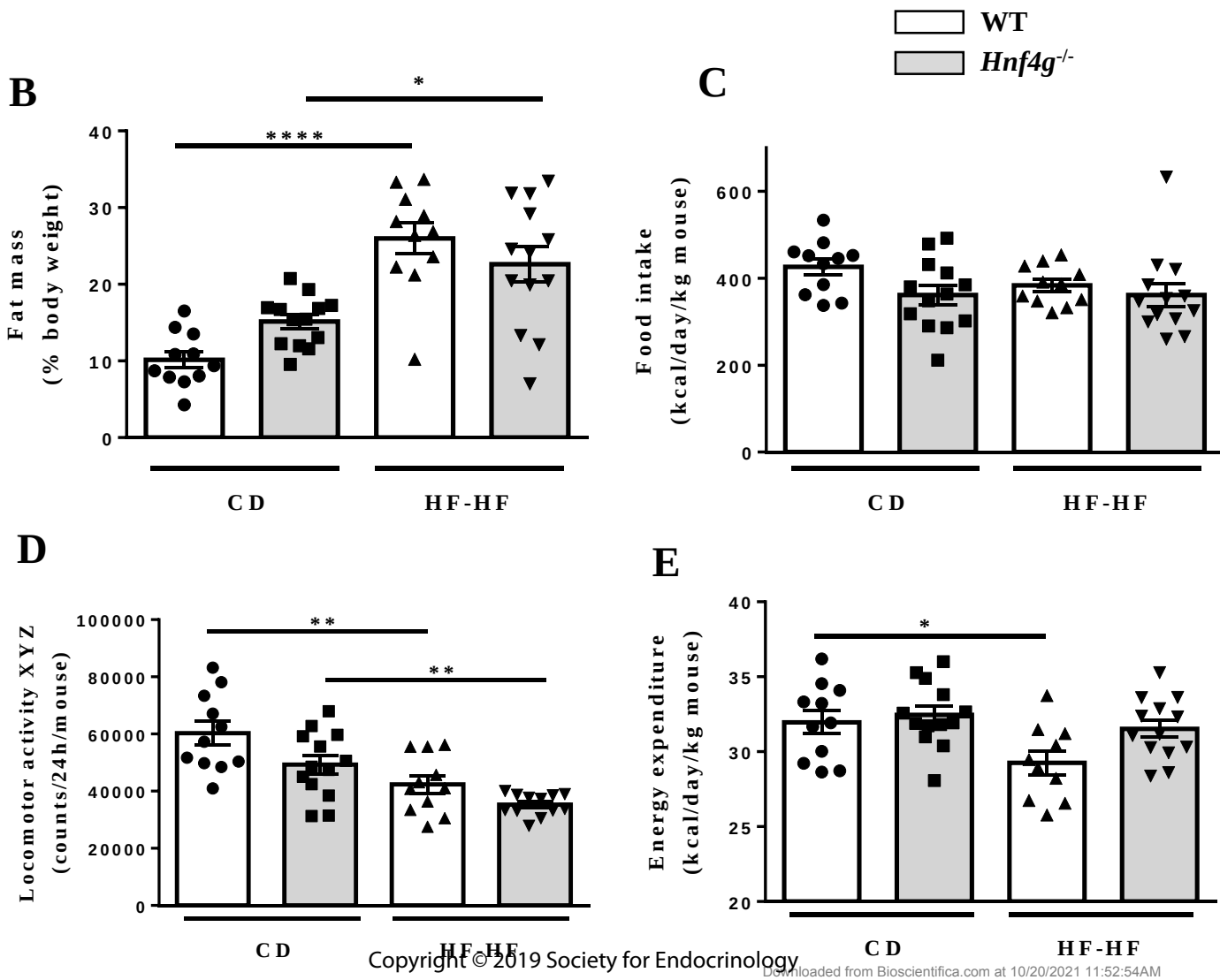

Figure 1, Ayari S & al

 Accepted Manuscript published as JOE-21-0092.R1. Accepted for publication: 12-Oct-2021

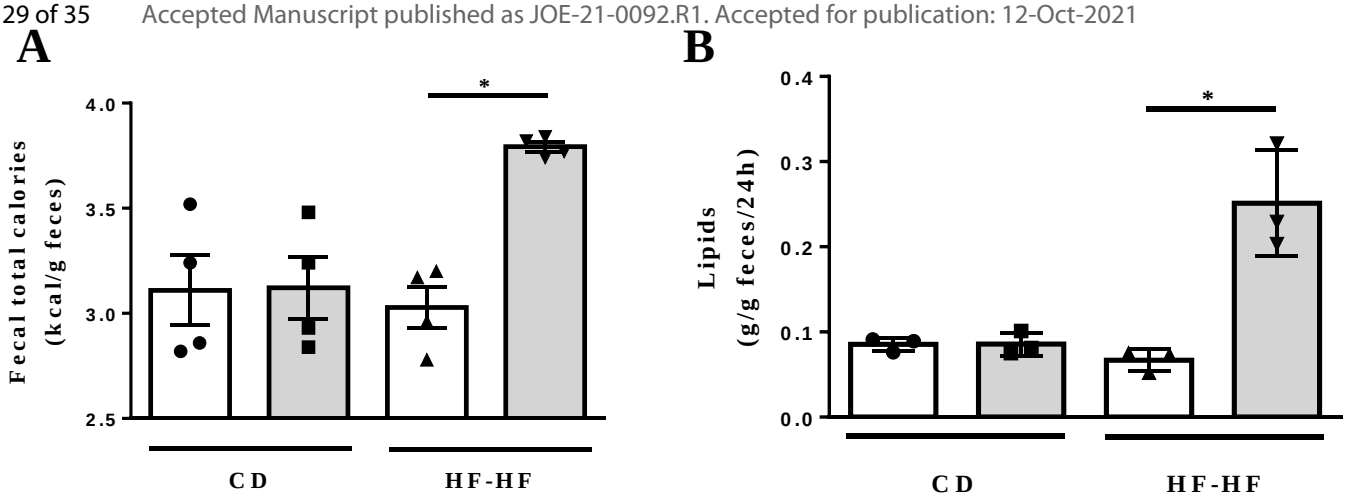

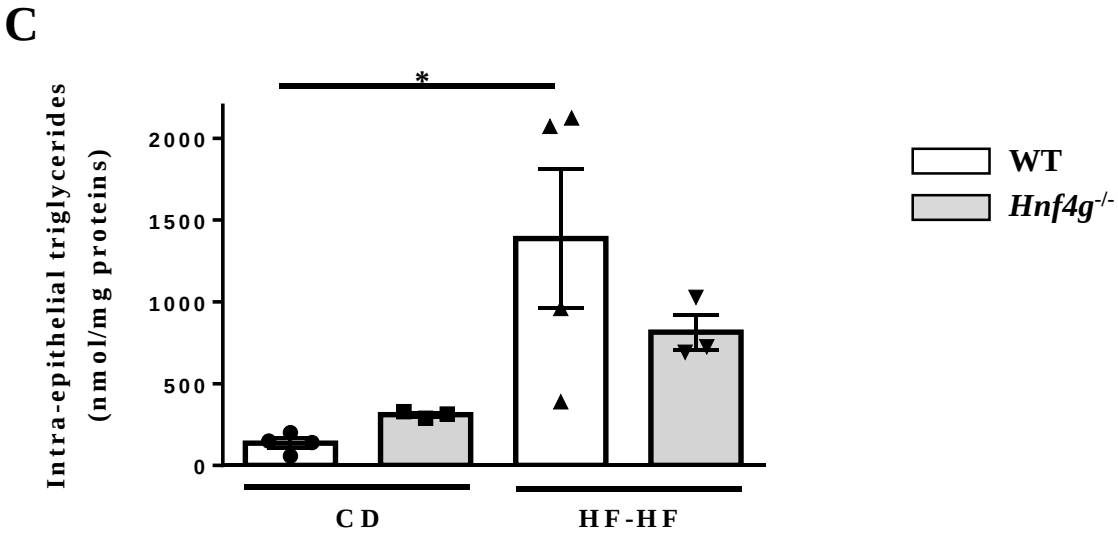

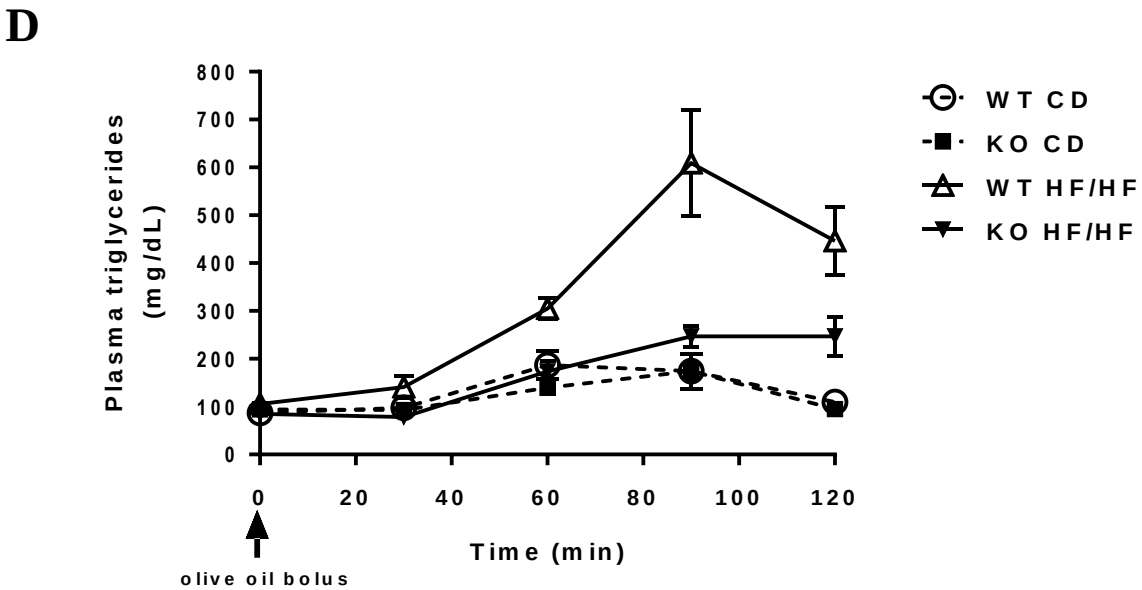

multiple comparison test	30 min	60 min	90 min	120 min
WT CD vs KO CD	ns	ns	ns	ns
WT HFHF vs KO HFHF	ns	ns	****	**
WT CD vs WT HF-HF	ns	ns	****	****
KO CD vs KO HF-HF	ns	ns	ns	*

Figure 2, Ayari S & al

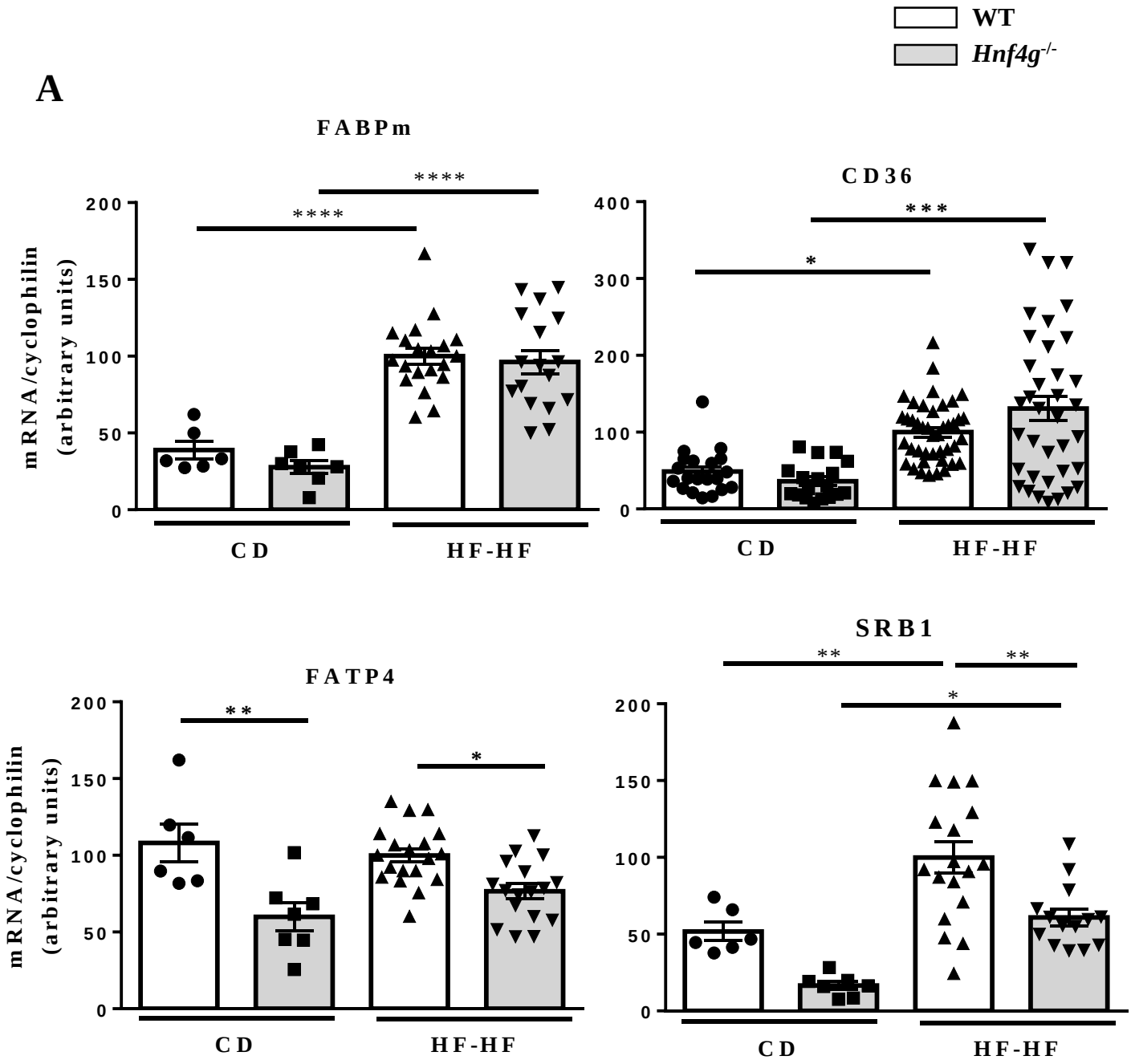

Figure 3, Ayari S & al

 Accepted Manuscript published as JOE-21-0092.R1. Accepted for publication: 12-Oct-2021

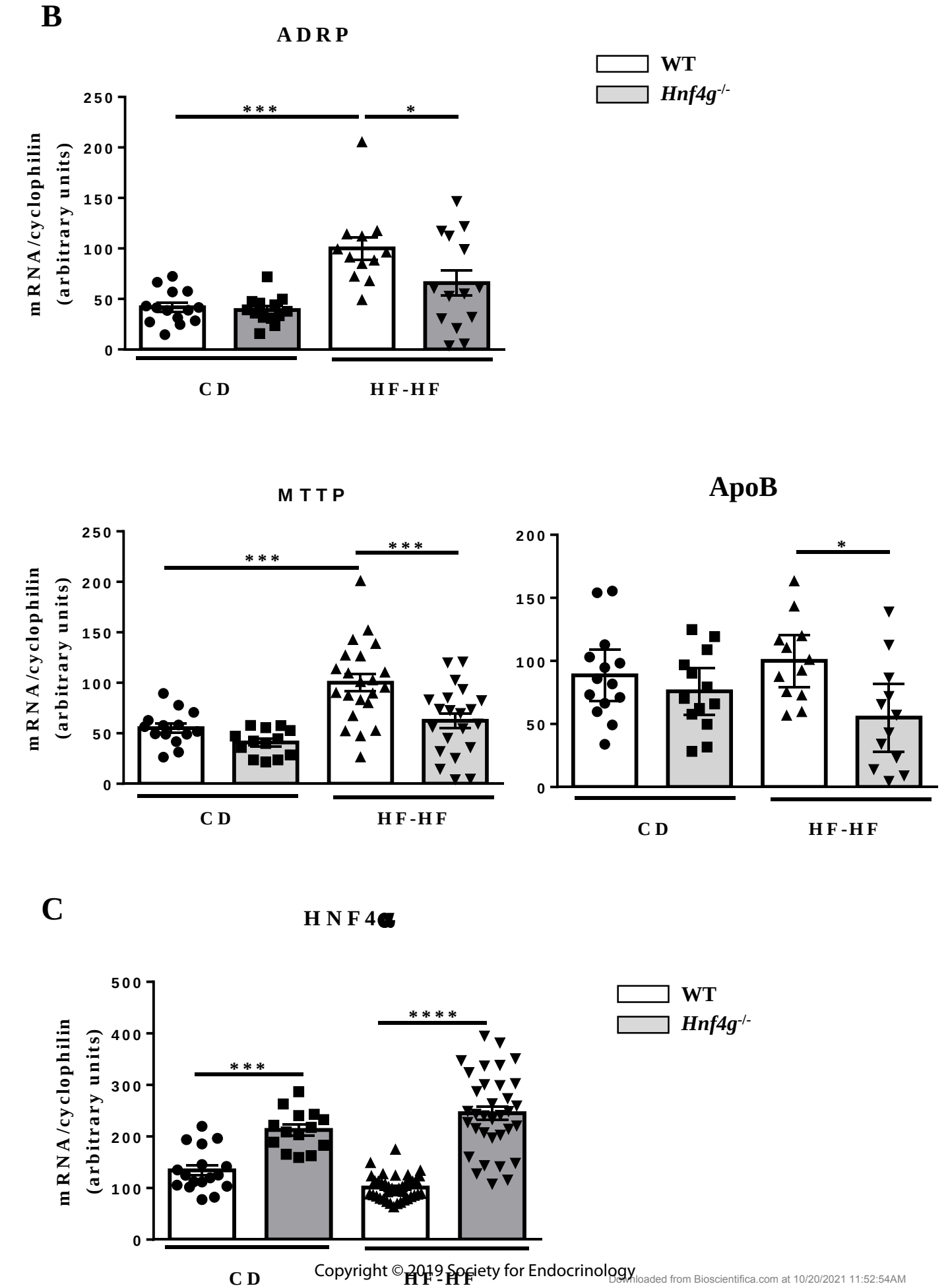

Figure 3, Ayari S & al

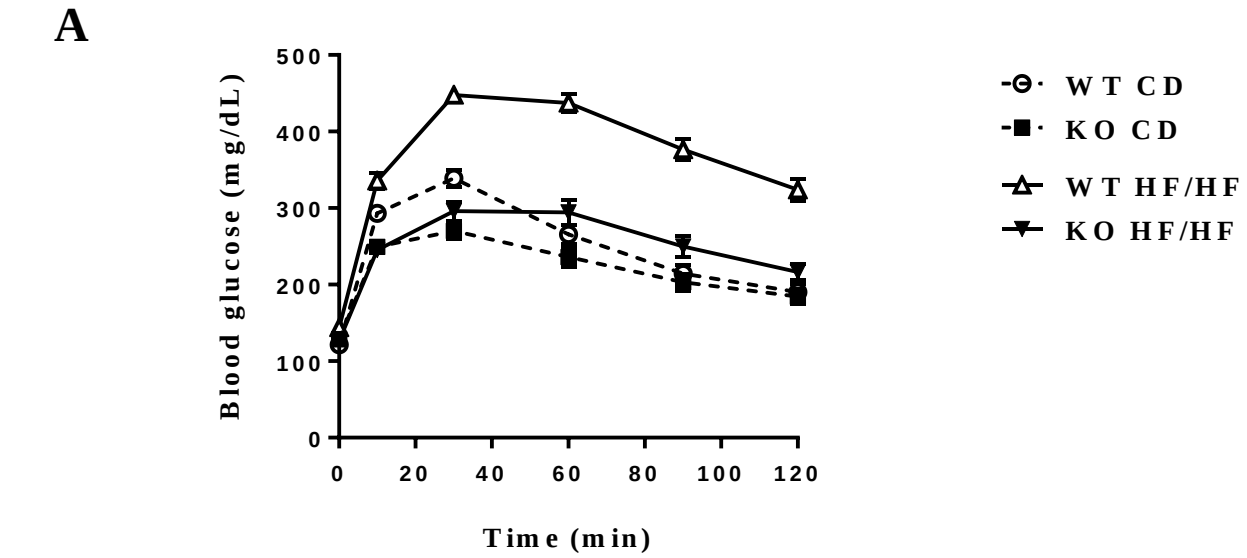

multiple comparison test	10 min	30 min	60 min	90 min	120 min
WT CD vs KO CD	*	****	ns	ns	ns
WT HFHF vs KO HFHF	****	****	****	****	****
WT CD vs WT HF-HF	*	****	****	****	****
KO CD vs KO HF-HF	ns	ns	**	*	ns

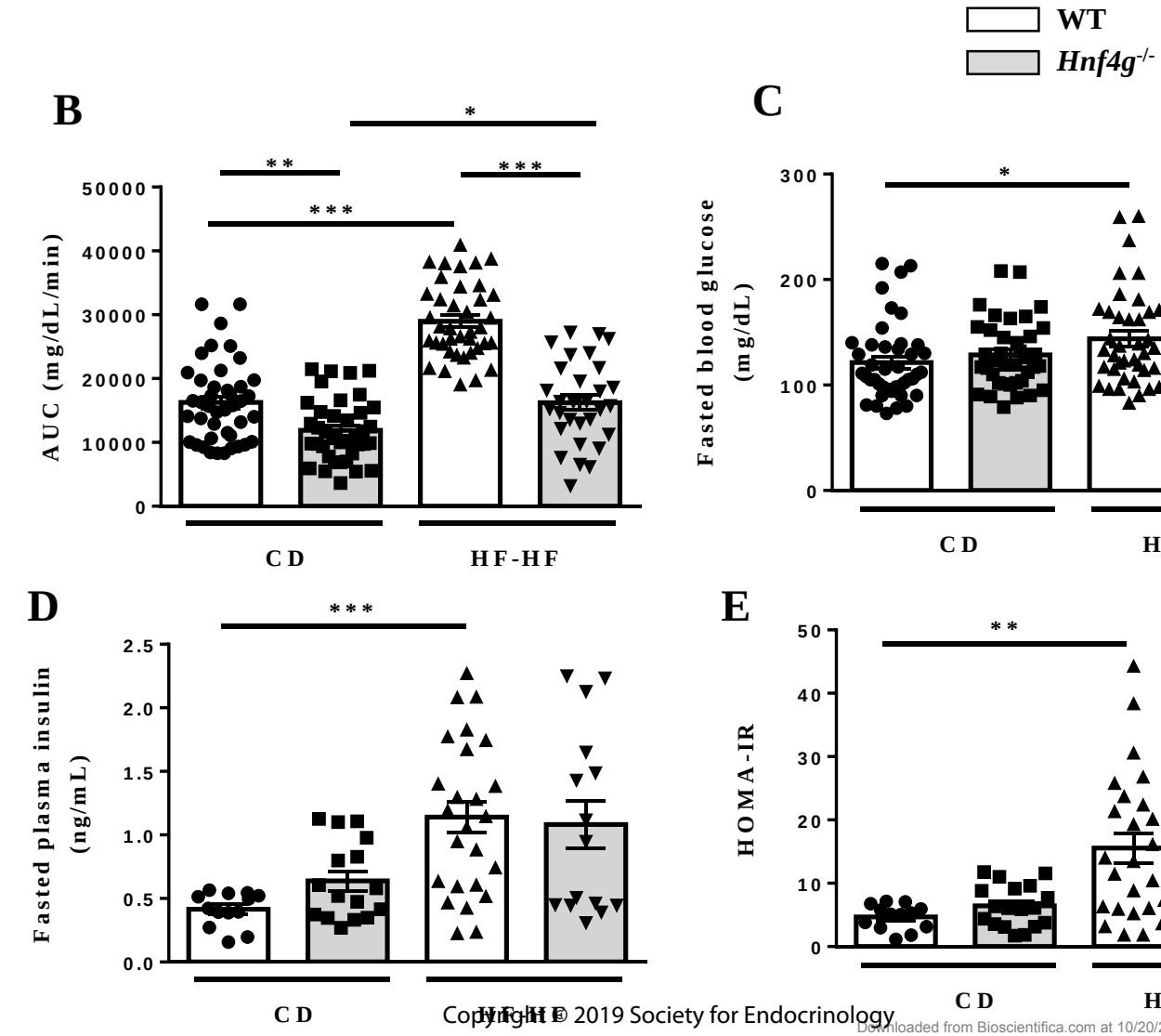

Figure 4, Ayari S & al

 Accepted Manuscript published as JOE-21-0092.R1. Accepted for publication: 12-Oct-2021

A

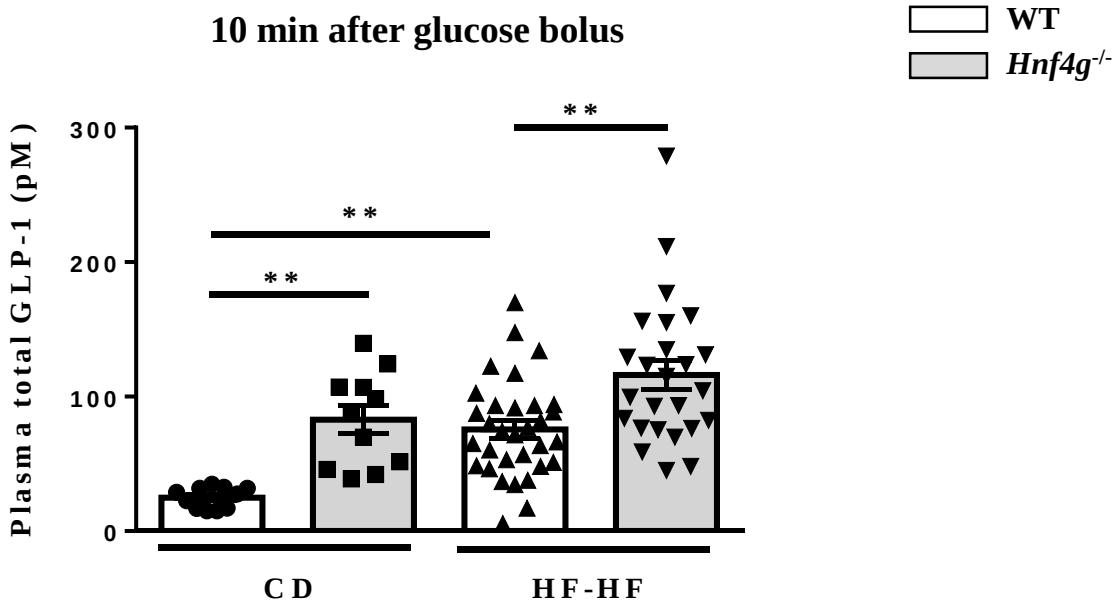

B

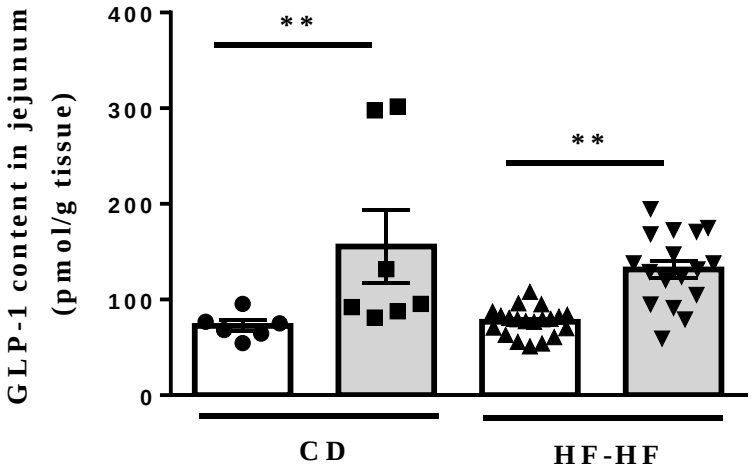

C

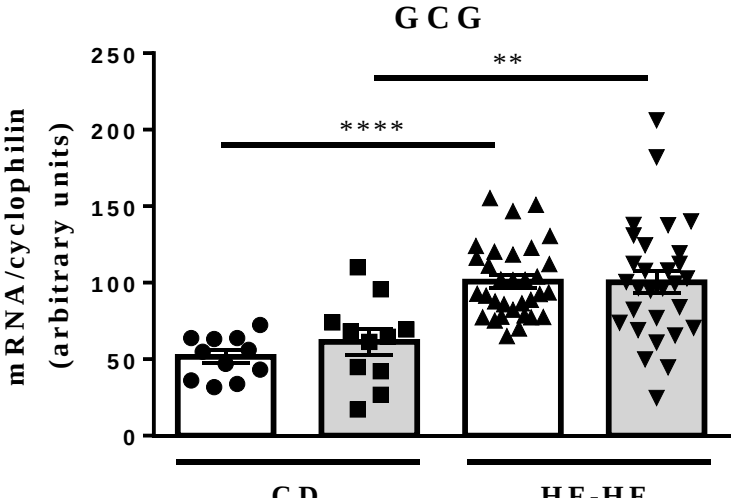

Figure 5, Ayari S & al

Table 1

Composition of control and high-fat diets

	Control diet (CD)	**High-Fat diet (HFD)**
Energy composition		
Proteins (Kcal %)	25.2	20
Lipids (Kcal %)	13.5	60
Carbohydrates (Kcal %)	61.3	20
Energy value		
(kcal / g)	3200	5240
Nutrient composition		
Proteins (%)	24.34	26.23
Lipids (%)	5.8	34.89
lard (%)		31.66
Carbohydrates (%)	43.11	25.04
starch (%)	38.1	
maltodextrine (%)		16.15
sugars (%)	4.55	
sucrose (%)		8.9
Fibers (%)	20.6	6.46
Minerals and vitamins	6.15	7.37

 Accepted Manuscript published as JOE-21-0092.R1. Accepted for publication: 12-Oct-2021

Table 2

Oligonucleotide sequences used for qPCR analysis

Gene name	Sequence (5' to 3')
cyclophilin	Fwd: GCCTTAGCTACAGGAGAGAA
	Rev: TTTCCTCCTGTGCCATCTC
fabpm	Fwd: ATGGCTGCTGCCTTTCAC
	Rev: GATCTGGAGGTCCCATTTCA
Srb1	Fwd: GCCCATCATCTGCCAACT
	Rev: TCCTGGGAGCCCTTTTTACT
Adrp	Fwd: CTCCACTCCACTGTCCACCT
	Rev: GCTTATCCTGAGCACCCTGA
Gcg	Fwd: CACGCCCTTCAAGACACAG
	Rev: GTCCTCATGCGCTTCTGTC
Apo B	Fwd: GCCCATTGTGGACAAGTTGATC
	Rev: CCAGGACTTGGAGGTCTTGGA
Mttp	Fwd: GGCAGTGCTTTTTCTCTGCT
	Rev: TGAGAGGCCAGTTGTGTGAC
CD36	Fwd: GCCAAGCTATTGCGACATGA
	Rev: ATCTCAATGTCCGAGACTTTTCAAC
Fatp4	Fwd: TATGGCTTCCCTGGTGTACTAT
	Rev: TTCTTCCGGATCACCACAGTC
Hnf4a	Fwd: CGTCCCTCGGCACTGTCC
	Rev: TCCTCCAGGCTCACTTGC